

ELECTROMAGNETIC FIELD GENERATED BY A HORIZONTAL ELECTRIC DIPOLE ON A DOUBLE NEGATIVE MEDIUM HALF SPACE

X.-Q. Zhu [†]

School of Electronic Engineering
Xidian University
Xi'an, Shaanxi 710071, China

W.-Y. Pan

China Research Institute of Radiowave Propagation
Qingdao, Shandong 266071, China

B.-R. Guan

The Institute of Antenna and Microwaves
Hangzhou Dianzi University
Hangzhou, Zhejiang 310018, China

Abstract—The electromagnetic field produced by a horizontal electric dipole over a double negative (DNG) medium half space is discussed, and the analytical expressions of the field which are convenient for calculation are derived. It can be concluded that the dipole on the configuration composed of the double positive (DPS) medium and the DNG medium half space can effectively excite the surface wave. The propagation wave number of the surface wave is less than that in both of the mediums, so that this kind of surface wave is a slow wave. Considered both the mediums are lossless, the amplitude of the surface wave decreases with the radial distance as $1/\rho^{1/2}$. The total field shows complicated interference because of the superposition of three kinds of wave modes.

Corresponding author: X.-Q. Zhu (xqzhu@sina.com).

[†] Also with China Research Institute of Radiowave Propagation, Qingdao, Shandong 266071, China.

1. INTRODUCTION

In 1968, Veselago was the first to consider double negative materials (DNG) with both negative permittivity and negative permeability [1]. It was predicted that the material would exhibit many unusual properties such as inverted Snell's law, Doppler shift and Cherenkov radiation. With the development of the fabricating technology of the DNG medium in recent years [2, 3], its distinctive physical characteristics have attracted considerable attention [4–7]. Moreover, it has been suggested that the material would have possible applications to the artificial dielectrics, lenses, antenna structure, optical and microwave components, sensors and frequency selective surface [8].

The frequency-domain electromagnetic field generated by an electric dipole near the boundary between two quite different material half-spaces has been investigated in the past decades owing to its wide ranging applications [9–18]. In addition, several groups have further studied the properties and applications of lateral pulses due to dipoles with delta-function and Gaussian pulse excitations in the time domain [18–23]. However, these works mainly focus on how the wave behaves along the boundary of two kinds of double positive medium (DPS), i.e., both permittivity and permeability are positive. Quite recently, the electromagnetic waves over half-space DNG metamaterials excited by a infinite line source and a space-time wave packet have been treated in [7, 8]. Some interesting results, such as backward lateral waves and a small negative displacement of the reflected wave have been found. Therefore, it is worthwhile to theoretically investigate the new properties and phenomena of the electromagnetic field excited by a dipole in a DNG medium.

The goal of the present paper is to study the characteristic of the electromagnetic field generated by a horizontal electric dipole on the interface of a DNG and DPS medium. The geometry and notation underlying analysis are shown in Fig. 1. The horizontal dipole is located on the upward-directed z -axis at a distance h from the origin of coordinates on the interface, i.e., the $\rho\phi$ -plane. The electromagnetic field is to be determined at an arbitrary point (ρ, ϕ, z) in cylindrical coordinate. The upper half space is region 1 with DPS medium, the lower half space is region 2 with DNG medium.

2. INTEGRATED FORMULAS OF THE FIELD

A time-harmonic dependence $e^{-i\omega t}$ is assumed and suppressed throughout. Following the procedure given in [19], the integral

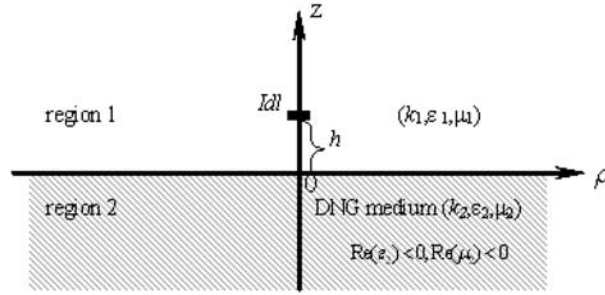


Figure 1. Geometry of a horizontal electric dipole in the half-space.

formulas of the electromagnetic field in region 1 are described by

$$\begin{aligned}
 E_{1\rho}(\rho, \phi, z) = & \frac{-\omega\mu_1 Idl}{4\pi k_1^2} \cos \phi \left(\int_0^\infty \left\{ k_1^2 J_0(\lambda\rho) - \frac{\lambda^2}{2} [J_0(\lambda\rho) - J_2(\lambda\rho)] \right\} \right. \\
 & \times \gamma_1^{-1} e^{i\gamma_1|z-h|} \lambda d\lambda + \int_0^\infty \left\{ \frac{\gamma_1 Q}{2} [J_0(\lambda\rho) - J_2(\lambda\rho)] \right. \\
 & \left. \left. - \frac{k_1^2 P}{2\gamma_1} [J_0(\lambda\rho) + J_2(\lambda\rho)] \right\} e^{i\gamma_1(z+h)} \lambda d\lambda \right) \quad (1)
 \end{aligned}$$

$$\begin{aligned}
 E_{1\phi}(\rho, \phi, z) = & \frac{\omega\mu_1 Idl}{4\pi k_1^2} \sin \phi \left(\int_0^\infty \left\{ k_1^2 J_0(\lambda\rho) - \frac{\lambda^2}{2} [J_0(\lambda\rho) + J_2(\lambda\rho)] \right\} \right. \\
 & \times \gamma_1^{-1} e^{i\gamma_1|z-h|} \lambda d\lambda + \int_0^\infty \left\{ \frac{\gamma_1 Q}{2} [J_0(\lambda\rho) + J_2(\lambda\rho)] \right. \\
 & \left. \left. - \frac{k_1^2 P}{2\gamma_1} [J_0(\lambda\rho) - J_2(\lambda\rho)] \right\} e^{i\gamma_1(z+h)} \lambda d\lambda \right) \quad (2)
 \end{aligned}$$

$$E_{1z}(\rho, \phi, z) = \frac{i\omega\mu_1 Idl}{4\pi k_1^2} \cos \phi \int_0^\infty \left(\pm e^{i\gamma_1|z-h|} + Q e^{i\gamma_1(z+h)} \right) \times J_1(\lambda\rho) \lambda^2 d\lambda \quad (3)$$

$$B_{1\rho}(\rho, \phi, z) = -\frac{\mu_1 Idl}{4\pi} \sin \phi \left(\int_0^\infty \pm J_0(\lambda\rho) e^{i\gamma_1|z-h|} \lambda d\lambda \right)$$

$$\begin{aligned}
& + \int_0^\infty \left\{ \frac{Q}{2} [J_0(\lambda\rho) + J_2(\lambda\rho)] \right. \\
& \left. - \frac{P}{2} [J_0(\lambda\rho) - J_2(\lambda\rho)] \right\} e^{i\gamma_1(z+h)} \lambda d\lambda \quad (4)
\end{aligned}$$

$$\begin{aligned}
B_{1\phi}(\rho, \phi, z) = & -\frac{\mu_1 I dl}{4\pi} \cos \phi \left(\int_0^\infty \pm J_0(\lambda\rho) e^{i\gamma_1|z-h|} \lambda d\lambda \right. \\
& + \int_0^\infty \left\{ \frac{Q}{2} [J_0(\lambda\rho) - J_2(\lambda\rho)] \right. \\
& \left. \left. - \frac{P}{2} [J_0(\lambda\rho) + J_2(\lambda\rho)] \right\} e^{i\gamma_1(z+h)} \lambda d\lambda \right) \quad (5)
\end{aligned}$$

$$B_{1z}(\rho, \phi, z) = \frac{i\mu_1 I dl}{4\pi} \sin \phi \int_0^\infty \left[e^{i\gamma_1|z-h|} - P e^{i\gamma_1(z+h)} \right] \gamma_1^{-1} J_1(\lambda\rho) \lambda^2 d\lambda \quad (6)$$

where $J_n(\lambda\rho)$ is the Bessel function of n th order, and the coefficients are defined as

$$Q = (k_1^2 \gamma_2 - k_2^2 \gamma_1) / (k_1^2 \gamma_2 + k_2^2 \gamma_1) \quad (7)$$

$$P = (\gamma_2 - \gamma_1) / (\gamma_2 + \gamma_1) \quad (8)$$

$$\gamma_1 = \sqrt{k_1^2 - \lambda^2} \quad (9)$$

$$\gamma_2 = -\sqrt{k_2^2 - \lambda^2} \quad (10)$$

$$k_i = \omega \sqrt{\varepsilon_i \mu_i}, \quad i = 1, 2 \quad (11)$$

For a DPS medium, both the real and imaginary parts of k are positive. However, for a DNG medium, the real part of k is negative and the imaginary one is positive.

3. EVALUATION OF THE INTEGRALS

Let us now evaluate the integrals (1)–(6). As an example, it is convenient to rewrite (1) as

$$E_{1\rho} = -\frac{\omega \mu_1 I dl}{4\pi k_1^2} \cos \phi [F_{\rho 0}(\rho, z-h) - F_{\rho 0}(\rho, z+h) + F_{\rho 1}(\rho, z+h)] \quad (12)$$

where $F_{\rho 0}(\rho, z - h)$, $F_{\rho 0}(\rho, z + h)$ and $F_{\rho 1}(\rho, z + h)$ are defined as, respectively

$$F_{\rho 0}(\rho, z - h) = \int_0^{\infty} \left\{ \frac{\gamma_1}{2} [J_0(\lambda\rho) - J_2(\lambda\rho)] + \frac{k_1^2}{2\gamma_1} [J_0(\lambda\rho) + J_2(\lambda\rho)] \right\} e^{i\gamma_1|z-h|} \lambda d\lambda \quad (13)$$

$$F_{\rho 0}(\rho, z + h) = \int_0^{\infty} \left\{ \frac{\gamma_1}{2} [J_0(\lambda\rho) - J_2(\lambda\rho)] + \frac{k_1^2}{2\gamma_1} [J_0(\lambda\rho) + J_2(\lambda\rho)] \right\} e^{i\gamma_1(z+h)} \lambda d\lambda \quad (14)$$

$$F_{\rho 1}(\rho, z + h) = \int_0^{\infty} \left\{ \frac{\gamma_1}{2} (Q + 1) [J_0(\lambda\rho) - J_2(\lambda\rho)] - \frac{k_1^2}{2\gamma_1} (P - 1) [J_0(\lambda\rho) + J_2(\lambda\rho)] \right\} e^{i\gamma_1(z+h)} \lambda d\lambda \quad (15)$$

(13) and (14) represent the direct and reflected wave, respectively, whose analytical results can be derived as [19]

$$F_{\rho 0}(\rho, z \pm h) = -k_1 e^{ik_1 r} \left[\frac{2k_1}{r^2} + \frac{2i}{r^3} + \frac{(z \pm h)^2}{r^2} \left(\frac{ik_1^2}{r} - \frac{3k_1}{r^2} - \frac{3i}{r^3} \right) \right] \quad (16)$$

in which, $r = r_1 = [\rho^2 + (z - h)]^{1/2}$ for plus is the path length of the direct wave, and $r = r_2 = [\rho^2 + (z + h)]^{1/2}$ for minus is the path length of the reflected wave. The third term $F_{\rho 1}(\rho, z + h)$ represents the surface and lateral wave influenced by the boundary surface of two mediums. When the distance between the observation and source point is large and it is greater than that of source or observation and boundary, the integral converges very slowly because of the high oscillatory of the Bessel functions. It is not easy to get exact values by numerical methods. Thus, it is necessary to evaluate the integral by using the complex function method. For the two DPS medium configuration, many authors have studied and derived its approximation expressions. When Medium 2 is a DNG material, the electromagnetic field excited by a vertical dipole is discussed in [24]. Borrowed from the idea of [24], the first integrand term of (15) has a singular point on the λ complex plane. It is quite different from that of two DPS configuration. However, the second integrand of (15) has no singular point on the λ

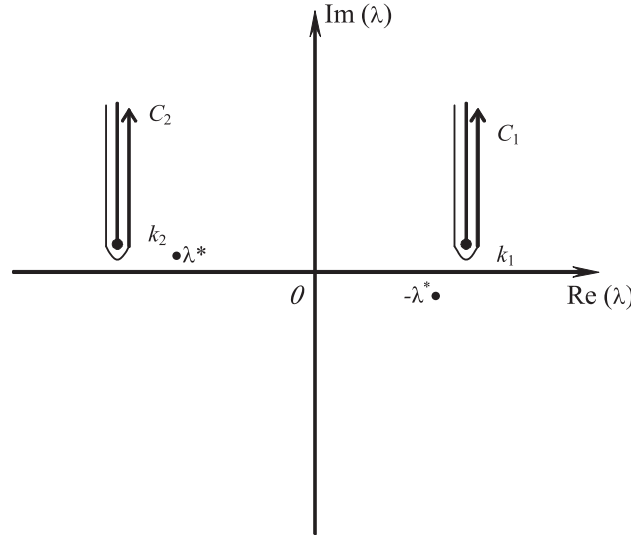


Figure 2. The configuration of the poles and the branch cuts.

complex plane. In addition, the integrand has two branch points at $\lambda = k_1$ and $\lambda = k_2$. In order to evaluate the integral in (15), it is necessary to shift the contour around the branch lines at $\lambda = k_1$ and $\lambda = k_2$. The configuration of poles and branch cuts is shown in Fig. 2. Using the similar procedure as in [24], $F_{\rho 1}(\rho, z + d)$ can be obtained by determining the poles and evaluating the integration along the branch cuts C_1 and C_2 .

$$\begin{aligned}
 F_{\rho 1}(\rho, z + h) &= \frac{-\omega\mu_1 I dl}{2\pi} \cos \phi \left(\frac{i\pi\gamma_1(\lambda^*)\gamma_2(\lambda^*)\lambda^*}{2N'(\lambda^*)} \right) \\
 &\quad \times e^{i\gamma_1(\lambda^*)(z+h)} \left[H_0^{(1)}(\lambda^*\rho) - H_2^{(1)}(\lambda^*\rho) \right] \\
 &\quad + \frac{k_1^2\gamma_{21}}{k_2^2} \sqrt{\frac{2}{k_1\pi\rho}} e^{ik_1r_2+i\pi/4} \left[\sqrt{\frac{\pi}{k_1\rho}} \right. \\
 &\quad \times \left(-\frac{e^{i\pi/4}(z+h)}{\sqrt{2}\rho} - A_1 \right) \\
 &\quad \left. + i\pi A_1^2 e^{-iP_d} \cdot \operatorname{erfc}(\sqrt{-iP_d}) \right] \left(1 + \frac{i}{k_1\rho} \right) \\
 &\quad + \frac{\pi}{\rho} \sqrt{\frac{1}{k_1\pi\rho}} e^{ik_1r_2+i\pi/2} e^{-iP_0} \operatorname{erfc}(\sqrt{-iP_0})
 \end{aligned}$$

$$-e^{i[k_2\rho+\gamma_{12}(z+h)]} \left[\frac{1}{k_2\rho^2} + \frac{i}{\gamma_{12}^2\rho^3} + \frac{i}{k_2^2\rho^3} \right] \quad (17)$$

where

$$\lambda^* = \frac{k_1 k_2}{\sqrt{k_1^2 + k_2^2}} \quad (18)$$

$$\gamma_1(\lambda^*) = \sqrt{k_1^2 - \lambda^{*2}} = \frac{k_1^2}{\sqrt{k_1^2 + k_2^2}} \quad (19)$$

$$\gamma_2(\lambda^*) = -\sqrt{k_2^2 - \lambda^{*2}} = -\frac{k_2^2}{\sqrt{k_1^2 + k_2^2}} \quad (20)$$

$$N'(\lambda^*) = -\left[\frac{k_2^2 \lambda^*}{\gamma_1(\lambda^*)} + \frac{k_1^2 \lambda^*}{\gamma_2(\lambda^*)} \right] = \frac{k_1^4 - k_2^4}{k_1 k_2} \quad (21)$$

$$A_1 = \frac{k_1 \gamma_{21}}{\sqrt{2} k_2^2 e^{i3\pi/4}} \quad (22)$$

$$-iP_d = \frac{-ik_1\rho}{2} \left[\frac{k_1 \gamma_{21}}{k_2^2} + \frac{z+h}{\rho} \right]^2 \quad (23)$$

$$-iP_0 = \frac{-ik_1\rho}{2} \left[\frac{\gamma_{21}}{k_1} + \frac{z+h}{\rho} \right]^2 \quad (24)$$

$$\gamma_{21} = -(k_2^2 - k_1^2)^{1/2} \quad (25)$$

$$\gamma_{12} = i(k_2^2 - k_1^2)^{1/2} \quad (26)$$

$$erfc(x) = 1 - \Phi(x) = \frac{2}{\sqrt{\pi}} \int_x^\infty e^{-t^2} dt \quad (27)$$

and $erfc(x)$ is the error function.

Similarly, the complete analytical expressions of the other components of the electromagnetic field can be obtained as follows:

$$\begin{aligned} E_{1\phi} = & \frac{\omega\mu_1 I dl}{2\pi} \sin\phi \left(-e^{ik_1 r_1} \left(\frac{i}{r_1} - \frac{1}{k_1 r_1^2} - \frac{i}{k_1^2 r_1^3} \right) \right. \\ & + e^{ik_1 r_2} \left(\frac{i}{r_2} - \frac{1}{k_1 r_2^2} - \frac{i}{k_1^2 r_2^3} \right) + \frac{i\pi\gamma_1(\lambda^*)\gamma_2(\lambda^*)\lambda^*}{2N'(\lambda^*)} \\ & \times e^{i\gamma_1(\lambda^*)(z+h)} \left[H_0^{(1)}(\lambda^*\rho) + H_2^{(1)}(\lambda^*\rho) \right] \\ & \left. - \frac{ik_1\gamma_{21}}{\rho k_2^2} \sqrt{\frac{2}{k_1\pi\rho}} e^{ik_1 r_2 + i\pi/4} \left[\sqrt{\frac{\pi}{k_1\rho}} \times \left(-\frac{e^{i\pi/4}(z+h)}{\sqrt{2}\rho} - A_1 \right) \right] \right) \end{aligned}$$

$$\begin{aligned}
& +i\pi A_1^2 e^{-iP_d} \cdot \operatorname{erfc}\left(\sqrt{-iP_d}\right) \Big] \\
& + \sqrt{\frac{\pi k_1}{\rho}} e^{ik_1 r_2} e^{-iP_0} \operatorname{erfc}\left(\sqrt{-iP_0}\right) \left(1 + \frac{i}{k_1 \rho}\right) \\
& + e^{i[k_2 \rho + \gamma_{12}(z+h)]} \left[\frac{k_2}{\gamma_{12}^2 \rho^2} + \frac{i}{\gamma_{12}^2 \rho^3} + \frac{i}{k_2^2 \rho^3} \right] \Big] \quad (28)
\end{aligned}$$

$$\begin{aligned}
E_{1z} = & \frac{-\omega \mu_1 I dl}{2\pi} \cos \phi \left(e^{ik_1 r_1} \left(\frac{ik_1}{r_1} - \frac{3}{r_1^2} - \frac{3i}{k_1 r_1^3} \right) \frac{\rho}{2k_1 r_1} \frac{z-h}{r_1} \right. \\
& - e^{ik_1 r_2} \left(\frac{ik_1}{r_2} - \frac{3}{r_2^2} - \frac{3i}{k_1 r_2^3} \right) \frac{\rho}{2k_1 r_2} \frac{z+h}{r_2} \\
& + \frac{\pi \gamma_2(\lambda^*) \lambda^{*2}}{2N'(\lambda^*)} e^{i\gamma_1(\lambda^*)(z+h)} H_1^{(1)}(\lambda^* \rho) \\
& - \frac{ik_1^2 \gamma_{21}}{k_2^2} \sqrt{\frac{1}{k_1 \pi \rho}} e^{ik_1 r_2} \left[\sqrt{\frac{\pi}{k_1 \rho}} \right. \\
& \left. - i\pi A_1 e^{-iP_d} \cdot \operatorname{erfc}\left(\sqrt{-iP_d}\right) \right] + \frac{e^{i[k_2 \rho + \gamma_{12}(z+h)]}}{\gamma_{12} \rho^2} \Big) \quad (29)
\end{aligned}$$

$$\begin{aligned}
B_{1\rho} = & \frac{-\mu_1 I dl}{2\pi} \sin \phi \left(-e^{ik_1 r_1} \frac{z-h}{2r_1} \left(\frac{ik_1}{r_1} - \frac{1}{r_1^2} \right) + e^{ik_1 r_2} \frac{z+h}{2r_2} \left(\frac{ik_1}{r_2} - \frac{1}{r_2^2} \right) \right. \\
& + \frac{i\pi k_1^2 \gamma_2(\lambda^*) \lambda^* e^{i\gamma_1(\lambda^*)(z+h)}}{2N'(\lambda^*)} \left[H_0^{(1)}(\lambda^* \rho) + H_2^{(1)}(\lambda^* \rho) \right] \\
& + \frac{k_1^2 \gamma_{21}}{\rho k_2^2} \sqrt{\frac{2}{k_1 \pi \rho}} e^{ik_1 r_2} \left[\sqrt{\frac{\pi}{k_1 \rho}} - i\pi A_1 e^{-iP_d} \cdot \operatorname{erfc}\left(\sqrt{-iP_d}\right) \right] \\
& + ik_1^2 \sqrt{\frac{2}{k_1 \pi \rho}} e^{ik_1 r_2 - i\pi/4} \left[\sqrt{\frac{\pi}{k_1 \rho}} \left(-\frac{e^{i\pi/4}(z+h)}{\sqrt{2}\rho} - C_1 \right) \right. \\
& \left. + C_1^2 i\pi e^{-iP_0} \cdot \operatorname{erfc}\left(\sqrt{-iP_0}\right) \right] \left(1 + \frac{i}{k_1 \rho} \right) \\
& + \frac{e^{i[k_2 \rho + \gamma_{12}(z+h)]}}{\gamma_{12} \rho} \left[\frac{k_2}{\rho} + \frac{i}{\rho^2} + \frac{ik_1^2}{k_2^2 \rho^2} \right] \Big) \quad (30)
\end{aligned}$$

$$\begin{aligned}
B_{1\phi} = & \frac{-\mu_1 Idl}{2\pi} \cos \phi \left(-e^{ik_1 r_1} \frac{z-h}{2r_1} \left(\frac{ik_1}{r_1} - \frac{1}{r_1^2} \right) + e^{ik_1 r_2} \frac{z+h}{2r_2} \left(\frac{ik_1}{r_2} - \frac{1}{r_2^2} \right) \right. \\
& + \frac{i\pi k_1^2 \gamma_2(\lambda^*) \lambda^* e^{i\gamma_1(\lambda^*)(z+h)}}{2N'(\lambda^*)} \left[H_0^{(1)}(\lambda^* \rho) - H_2^{(1)}(\lambda^* \rho) \right] \\
& - \frac{ik_1^3 \gamma_{21}}{k_2^2} \sqrt{\frac{1}{k_1 \pi \rho}} e^{ik_1 r_2} \left[\sqrt{\frac{\pi}{k_1 \rho}} - i\pi A_1 e^{-iP_d} \operatorname{erfc} \left(\sqrt{-iP_d} \right) \right] \\
& \times \left(1 + \frac{i}{k_1 \rho} \right) + \frac{ik_1}{\rho} \sqrt{\frac{2}{k_1 \pi \rho}} e^{ik_1 r_2 - i3\pi/4} \left[\sqrt{\frac{\pi}{k_1 \rho}} \left(-\frac{e^{i\pi/4}(z+h)}{\sqrt{2}\rho} - C_1 \right) \right. \\
& \left. + C_1^2 i\pi e^{-iP_0} \cdot \operatorname{erfc} \left(\sqrt{-iP_0} \right) \right] \\
& \left. + \frac{e^{i[k_2 \rho + \gamma_{12}(z+h)]}}{\gamma_{12} \rho} \left[-\frac{k_1^2}{k_2 \rho} + \frac{ik_1^2}{k_2^2 \rho^2} - \frac{i}{\rho^2} \right] \right) \quad (31)
\end{aligned}$$

$$\begin{aligned}
B_{1z} = & \frac{-\mu_1 Idl}{2\pi} \sin \phi \left\{ e^{ik_1 r_1} \left(\frac{ik_1}{r_1} - \frac{1}{r_1^2} \right) \frac{\rho}{2r_1} - e^{ik_1 r_2} \left(\frac{ik_1}{r_2} - \frac{1}{r_2^2} \right) \frac{\rho}{2r_2} \right. \\
& \left. - \frac{i}{\rho^2} \sqrt{\frac{\pi}{k_1 \rho}} e^{ik_1 r_2} e^{-iP_0} \cdot \operatorname{erfc} \left(\sqrt{-iP_0} \right) \right\} - \frac{k_2^2 e^{i[k_2 \rho + \gamma_{12}(z+h)]}}{\gamma_{12}^2 \rho^2} \quad (32)
\end{aligned}$$

where

$$C_1 = \frac{\gamma_{21}}{\sqrt{2} k_1 e^{i3\pi/4}} \quad (33)$$

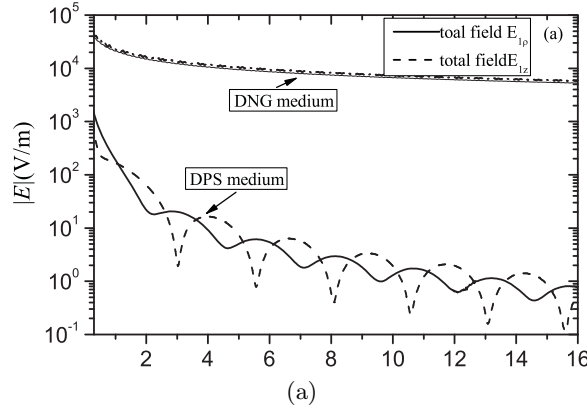
4. NUMERICAL RESULTS AND DISCUSSION

Thus, the complete analytical expressions of the electromagnetic field in the DPS medium excited by a horizontal dipole over the boundary of DPS and DNG mediums have been derived when $|k\rho| \gg 1$, $\rho \gg h$ and $\rho \gg |z|$. As an example, each term in (17) is discussed to explain its physical conception. The first term indicates the surface wave propagating along the boundary of two different mediums. Its wave number is given by (18) and determined by the excited wave frequency and the physical parameters of two mediums. When Medium 1 is air and $|k_2| > k_1$, it can be seen from (18) that $|\lambda^*|$ is smaller than the wave number in Medium 1, so it is a kind of slow wave. As the distance between the observation and source point becomes large, the phase of the surface wave decreases and its amplitude for the lossless media attenuates as $1/\rho^{1/2}$ due to $H_n^{(1)}(\lambda^* \rho) \approx [2/(\pi \lambda^* \rho)]^{1/2} e^{i(\lambda^* \rho - \pi/4) - in\pi/2}$. In z direction, the surface wave decreases with $e^{i\gamma_1(\lambda^*)(z+h)}$. The

variation of surface wave with z is more slowly than that in ρ direction because $\gamma_1(\lambda^*)$ is much smaller than k_1 as $|k_2| \gg k_1$. The second and third terms indicate the lateral wave propagating with $e^{ik_1\rho}$ in Medium 1 along the surface. The fourth term represents the lateral wave propagating with $e^{ik_2\rho}$ in Medium 2. Because the real part of k_2 is negative, its phase decreases with ρ . As the Medium 2 is lossy, it attenuates very quickly as the radial distance.

According to formulas (16)–(33) given above, we have performed our numerical calculations for the electric field components and its sub-components. The physical parameters used in our calculations are chosen as $f = 1.2$ GHz, $I dl = 1$ (A·m), $z = h = 0$. For convenience, the contribution of k_1 wave in the following figures is the sum of the direct, reflective and lateral waves in Medium 1. The contribution of k_2 wave indicates the lateral wave in Medium 2.

The amplitude of the electric field $E_{1\rho}(\rho, 0, 0)$ and $E_{1z}(\rho, 0, 0)$ has been numerically calculated as a function of propagation distance with $\varepsilon_{1r} = \mu_{1r} = 1$ and $\varepsilon_{2r} = \mu_{2r} = -1.1$. The total field and its sub-components of $E_{1\rho}$ are illustrated in Figs. 3(a) and 3(b), respectively. Moreover, the calculation results for $\varepsilon_{2r} = 1.21$, $\mu_{2r} = 1$ are also given in Fig. 3(a). It can be seen that (1) The variation of the amplitude of $E_{1\rho}$ with the distance is similar to that of E_{1z} at $\phi = 0$. Compared with the electric field component, the magnetic field component is so small that it is neglected in Fig. 2; (2) The surface wave can be effectively excited by the horizontal dipole in the surface of DPS and DNG mediums. Because of the contribution of the surface wave, the total field in this configuration is greater than that of two DPS medium configuration; (3) Because amplitude of the surface wave varies with radial distance as $\rho^{-1/2}$, the contribution of the surface wave to the total field plays an important role for sufficiently large values of ρ . As ρ



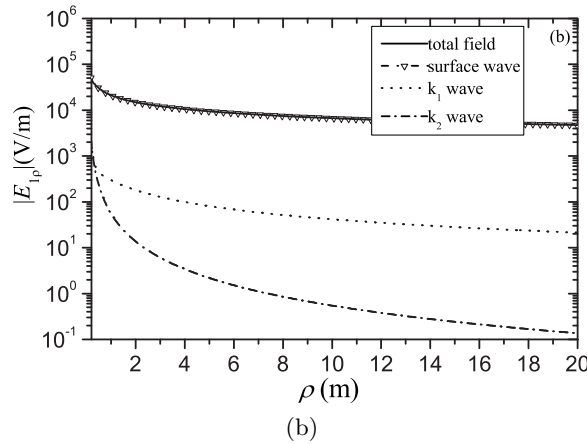


Figure 3. The electric field $E_{1\rho}(\rho, 0, 0)$ and its sub-components as a function of the distance.

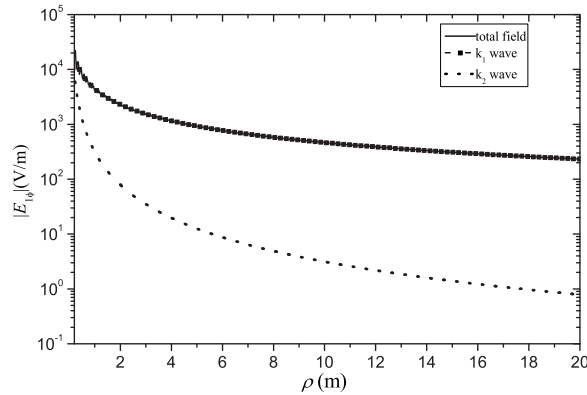


Figure 4. The electric field $E_{1\phi}(\rho, \pi/2, 0)$ and its sub-components as a function of the distance.

increases, the second term in (17) reduces to $e^{ik_1\rho}[1/(k_1\rho^2) + i/(k_1^2\rho^3)]$, thus the lateral wave in Medium 1 decreases approximately as $1/(k_1\rho^2)$. However, the lateral wave in Medium 2 decreases approximately as $1/(k_2\rho^2)$. Therefore, the contribution of lateral wave in Medium 1 is greater than that in Medium 2 and attenuates slowly with the radial distance.

The electric field $E_{1\phi}(\rho, \pi/2, 0)$ as a function of propagation distance is given in Fig. 4 with the same physical parameters as in Fig. 3. The total field comes mainly from the contribution of the

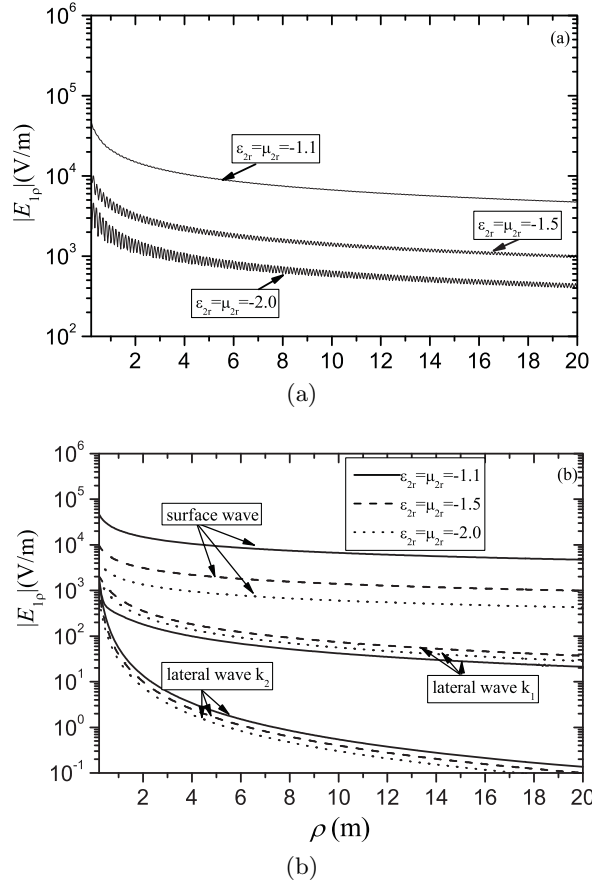


Figure 5. The electric field $E_{1\rho}(\rho, 0, 0)$ and its sub-components as a function of the distance.

lateral wave in Medium 1. The lateral wave in Medium 2 decreases quickly with the propagation distance. The contribution of the surface wave is smaller than that of lateral wave and is ignored. Moreover, the amplitude of the magnetic field component $B_{1\rho}(\rho, \pi/2, 0)$ and $B_{1z}(\rho, \pi/2, 0)$ is much smaller than that of the electric field.

To study the effect of the physical parameter of Medium 2 on the amplitude of the field, the variation of the field component $E_{1\rho}(\rho, 0, 0)$ with the distance is calculated at $\epsilon_{2r} = \mu_{2r} = -1.1, -1.5, -2.0$, respectively. Figs. 5(a) and 5(b) show the total field and its sub-components, respectively. It is shown that the total field decreases as the amplitude of relative permittivity and permeability of Medium 2 increases. It is mainly induced by the variation of contribution of

the surface wave with the physical parameters of the DNG medium. Because of the existing of three kinds of wave number, the total field shows complicated interference.

5. CONCLUSION

In this paper, the complete analytical expressions have been derived for the electromagnetic field generated by a horizontal electric dipole over the interface of the DPS and DNG mediums. Numerical calculations of the field components are performed and illustrated when both the dipole and observation point are located on the interface of two mediums. The influence of the physical parameters on the fields is also calculated and discussed. The main conclusions obtained in the present paper are summarized as follows.

- (1) Comparing with the electromagnetic field induced by a horizontal dipole on the interface of two DPS material, the surface wave can be effectively excited on the interface of a DPS and DNG medium. The wave number of the surface wave is less than the wave number in Region 1 and Region 2, so that this kind of surface wave is a kind of slow wave, the amplitude of the surface wave for the lossless media decreases with the radial distance as $1/\rho^{1/2}$. The variation of the surface wave in the vertical direction of the interface is much more slowly than that in the radial direction as $|k_2| \gg k_1$.
- (2) The excited field is the superposition of the contribution of the direct, reflected, lateral and surface waves with three kinds of propagation wave numbers. The total field shows complicated interference because of the superposition of those waves.
- (3) When the upper half space is air, the amplitudes of field components $E_{1\rho}$, E_{1z} and $B_{1\varphi}$ depend mainly on the contributions of surface wave, whose wave number is influenced by the physical parameters of the DNG medium in the lower half space. However, the contributions of the lateral waves play important role for the amplitudes of field components $E_{1\varphi}$, $B_{1\rho}$ and B_{1z} .

REFERENCES

1. Veselago, V. G., "The electrodynamics of substances with simultaneously negative values of ε and μ ," *Sov. Phys. Usp.*, Vol. 10, No. 4, 509–514, 1968.
2. Shelby, A., D. R. Smith, and S. Schultz, "Experimental verification of a negative index of refraction," *Science*, Vol. 292, No. 5514, 77–79, 2001.

3. Simovski, C. R. and B. Sauviac, "Toward creating isotropic microwave composites with negative refraction," *Radio Sci.*, Vol. 39, No. 2, Rs2014.1–Rs2014.18, 2004.
4. Caloz, C., A. Sanada, and T. Itoh, "Microwave applications of transmission line based negative refraction index structures," *2003 Asia Pacific Microwave Conference*, 2003.
5. Grbic, A. and G. V. Eleftheriades, "Subwavelength focusing using a negative-refractive-index transmission line lens," *IEEE Antennas and Wireless Propagation Letters*, Vol. 2, 186–189, 2003.
6. Baccarelli, P., P. Burghignoli, and S. Paulotto, "Surfacewave suppression in a double-negative metamaterial grounded slab," *IEEE Antennas and Wireless Propagation Letters*, Vol. 2, 269–272, 2003.
7. Thomas, J. R. and A. Ishimaru, "Wave packet incident on negative-index media," *IEEE Transactions on Antennas and Propagation*, Vol. 53, No. 3, 1591–1599, 2005.
8. Ishimaru, A., J. R. Thomas, and S. Jaruwatanadilok, "Electromagnetic waves over half-space metamaterials of arbitrary permittivity and permeability," *IEEE Transactions on Antennas and Propagation*, Vol. 53, No. 3, 915–921, 2005.
9. Sommerfeld, A., "Propagation of waves in wireless telgraphy," *Ann. Phys.*, Vol. 28, 665–736, 1909.
10. Sommerfeld, A., "Propagation of waves in wireless telgraphy," *Ann. Phys.*, Vol. 81, 1135–1153, 1926.
11. Wait, J. R., *Electromagnetic Wave in Stratified Media*, Pergamon Press, London, 1962.
12. Banos, A. J., *Dipole Radiation in the Presence of a Conducting Half-space*, Pergamon press, Oxford, 1966.
13. King, R. W. P., "New formulas for the electromagnetic field of a vertical electric dipole in a dielectric or conducting half-space near its horizontal interface," *J. Appl. Phys.*, Vol. 53, 8476–8482, Dec. 1982.
14. Wu, T. T. and King, R. W. P., "Lateral waves: A new formula and interference pattern," *Radio Sci.*, Vol. 17, No. 3, 521–531, 1982.
15. Wu, T. T. and R. W. P. King, "Lateral waves: New formulas for $E_{1\phi}$ and E_{1z} ," *Radio Sci.*, Vol. 17, No. 3, 532–538, 1982.
16. King, R. W. P. and T. T. Wu, "Lateral waves: New formulas for the magnetic field," *J. Appl. Phys.*, Vol. 54, No. 2, 507–514, 1983.
17. King, R. W. P. and M. F. Brown, "Lateral electromagnetic waves along plane boundaries: A summarizing approach," *Proc. IEEE*,

- Vol. 72, No. 5, 595–611, 1984.
18. King, R. W. P., “Electromagnetic surface waves: New formulas and applications,” *IEEE Trans. Antennas Propag.*, Vol. 33, No. 11, 1204–1212, 1985.
 19. King, R. W. P., O. Margaret, and T. T. Wu, *Lateral Electromagnetic Wave*, Springer-verlag Press, 1992.
 20. Wu, T. T. and R. W. P. King, “Lateral electromagnetic pulses generated by a vertical electric dipole on the boundary between two dielectric,” *J. Appl. Phys.*, Vol. 62, 4345–4355, Dec. 1987.
 21. King, R. W. P., “Lateral electromagnetic pulses generated by a vertical electric dipole on a plane boundary between dielectric,” *J. Electro. Waves Appl.*, Vol. 2, No. 3–4, 225–243, 1988.
 22. King, R. W. P., “Lateral electromagnetic pulses generated on a plane boundary between dielectrics by vertical and horizontal dipole source with Gaussian pulse excitation,” *J. Electro. Waves Appl.*, Vol. 2, 589–597, 1989.
 23. Li, K., Y. L. Lu, and M. H. Li, “Approximate formulas for lateral electromagnetic pulses from a horizontal dipole on the surface of one-dimensionally anisotropic medium,” *IEEE Trans. Antennas Propag.*, Vol. 53, No. 3, 933–937, 2005.
 24. Zhu, X. Q., W. Y. Pan, and B. R. Guan, “The electromagnetic field produced by a vertical electric dipole on a negative-index media half space,” *Chinese Journal of Radio Science*, Vol. 21, No. 2, 177–183, 2006.